# Nonreciprocal propagation of surface waves in quasiperiodic superlattices

B. L. Johnson
*Department of Physics, University of Colorado, Boulder, Colorado 80309-0390*

R. E. Camley
*Department of Physics, University of Colorado, Colorado Springs, Colorado 80933-7150*
(Received 19 November 1990)

We investigate the dispersion relations and amplitude profiles of magnetoplasmons in semi-infinite superlattices, the unit cells of which are composed of two different thicknesses of bilayer minicells arranged in a Fibonacci sequence. We find that there exists another spectrum of both bulk and surface modes in the quasiperiodic structure, which is not present in the periodic structure. These surface modes become nonreciprocal with respect to the direction of propagation in an applied magnetic field. Since the number and frequency of these modes depend upon the layering of the unit cell, and since the surface modes are nonreciprocal, our results could be important to surface-wave-device applications.

## I. INTRODUCTION

There has been considerable interest recently in the properties of quasiperiodic structures. Theoretical investigations have focused on one-dimensional Schrödinger equations with two values of (constant) potentials arranged in a quasiperiodic sequence,[1-4] and superlattices with two thicknesses of films arranged in a quasiperiodic sequence.[5-9] The quasiperiodicity in the potentials or the superlattice layering has been imposed analytically by requiring that these parameters follow a Fibonacci sequence, i.e., if a system is constructed of building blocks $\alpha$ and $\beta$, then the system will be a sequence of blocks which obeys the recursion relation $F_m = F_{m-1} + F_{m-2}$, for integer $m \geq 3$, with $F_1 = \{\alpha\}$ and $F_2 = \{\alpha\beta\}$. To illustrate the procedure, then, the next iteration produces $F_3 = \{\alpha\beta\alpha\}$. Therefore we see that the extended sequence will be $\{\alpha\beta\alpha\alpha\beta\alpha\beta\alpha \cdots\}$. If the sequence is the simple Fibonacci sequence represented above, where each term is the sum (or concatenation) of its two immediate predecessors, then the ratio of the number of elements, $n_\alpha n_\beta$, approaches the golden mean $g = (1+\sqrt{5})/2$ as $m \to \infty$. Although we will employ the simple sequence given above, other types of sequences have also been studied.[4]

Two broad types of techniques have been employed in studying these structures. The first work involved finding the allowed bands of energy in the Schrödinger equation model,[1] or the allowed susceptibilities for plasmons in a superlattice,[5] given a set of initial conditions. The general results of this type of work show that the allowed bands form a Cantor set as $m \to \infty$. The properties of these solutions have been studied in detail. The other type of calculation involves assuming a model for the susceptibility (superlattice), and calculating the dispersion for the elementary excitations in the quasiperiodic structure,[8] or the Raman spectra.[6] The results of these studies also show multiplicity in the band structure as a direct result of the quasiperiodicity.

In this paper, we will examine the effects of quasiperiodic layering on magnetoplasmons. We will examine both bulk and surface excitations, and in particular, we will examine the effects of an applied magnetic field on the new modes generated by the quasiperiodic layering. We assume that the magnetic field is applied parallel to the interfaces. The results could be important for device applications, since we expect many of the new surface modes to be nonreciprocal with respect to direction of propagation.[10]

In particular, we will show that, in a specific model, each mode (or band of modes) which exists in the periodic superlattice will be split in the quasiperiodic structure. The number of additional modes is dictated by the Fibonacci *number* which corresponds to the integer $m$ given above. For instance, if $G_M = G_{m-1} + G_{m-2}$, for $m \geq 2$, with $G_0 = G_1 = 1$, then the number of additional, modes (bands) corresponding to $m = 3$ is $G_3 = 3$. The particular model with which we will be concerned is a semi-infinite, periodic array of unit cells, where the unit cell contains a sequence of $F_m$ alternating bilayers (minicells) of two different thicknesses, using the procedure described above to create the layering sequence. To make the calculation tractable, we will consider a unit cell configured in the $F_3 = \{\alpha\beta\alpha\}$ manner. The superlattice will therefore look like $\{\alpha\beta\alpha\alpha\beta\alpha\alpha\beta\alpha\alpha\beta\alpha\alpha\beta\alpha \cdots\}$. Although this model is in reality periodic, the extended case (semi-infinite) provides an adequate representation of the major features present in the actual quasiperiodic structure.[4]

To understand how the multiplicity of allowed modes might occur for a different layering arrangement, we consider the following argument. In the case of plasmons, we know that the collective superlattice excitations, both bulk and surface, are a coupled set of surface excitations on the individual films. Therefore we might expect the number of modes (or bands) to be related to the number of *distinct active layers* (layers containing free charges) within the unit cell, the main idea being that each distinct layer within a unit cell will support an odd-even pair of

 

surface modes, each of which is in turn coupled to neighboring unit cells via Bloch's theorem. We will show that this is indeed the case by examining the plasmon amplitude profiles for selected modes of the structure.

The rest of the paper is organized as follows. In Sec. II we develop the theory for calculating the bulk and surface dispersion relations for magnetoplasmons in a superlattice where the unit cell has $G_m$ bilayers. In Sec. III we give numerical results for a particular geometry, given by $G_3=3$ bilayers/(unit cell). Finally, we summarize the results in Sec. IV.

## II. THEORY

In this section, we present the general theory for calculating the bulk and surface plasmon dispersion relations for a semi-infinite, quasiperiodic superlattice in the presence of a static magnetic field applied parallel to the material interfaces. We consider a periodic array of unit cells, where a unit consists of a Fibonacci sequence of two different thicknesses of bilayers (labeled $\alpha$ and $\beta$), as discussed in Sec. I. A bilayer will be defined as a composite of two films of materials $A$ and $B$, respectively.

We let the $y$ axis point into the structure, while the magnetic field lies along the $z$ direction (see Fig. 1). We will consider propagation along the $x$ axis, perpendicular to the applied field.

If we make the assumption that only material $A$ contains free charges (material $B$ is an insulator), then we may write the dielectric functions of the materials as follows. In the geometry of Fig. 1,

$$\epsilon_A=\begin{bmatrix}\epsilon_1 & i\epsilon_2 & 0\\ -i\epsilon_2 & \epsilon_1 & 0\\ 0 & 0 & \epsilon_3\end{bmatrix},\quad \epsilon_B=\epsilon_{\infty B}\overleftrightarrow{I} \tag{2.1}$$

where

$$\begin{aligned}\epsilon_1&=\epsilon_{\infty A}[1+\omega_p^2/(\omega_c^2-\omega^2)]\ ,\\ \epsilon_2&=\epsilon_{\infty A}\omega_c\omega_p^2/\omega(\omega_c^2-\omega^2)\ ,\\ \epsilon_3&=\epsilon_{\infty A}[1-\omega_p^2/\omega^2]\ ,\end{aligned} \tag{2.2}$$

and where $\omega_p$ is the plasma frequency, $\omega_c$ is the cyclotron frequency $eB/m^*c$, and the $\infty$ subscript refers to the background dielectric constant of the given material. If we assume that material $A$ is simply material $B$ with doping, then we may drop the additional subscript $(A,B)$ on the background dielectric constants given in Eq. (2.2).

In the long-wavelength, static approximation, we have $\nabla\times\mathbf{E}=\mathbf{0}$, which allows us to introduce a scalar potential $\phi$ given by $\mathbf{E}=-\nabla\phi$. Using this and the relationship $\mathbf{D}=\epsilon\mathbf{E}$, we find

$$\nabla\cdot\mathbf{D}=\epsilon_1\left[\frac{\partial^2}{\partial x^2}+\frac{\partial^2}{\partial y^2}\right]\phi+\epsilon_3\frac{\partial^2}{\partial z^2}\phi=0\ . \tag{2.3}$$

Since we are considering only propagation along $x$, $\phi$ is independent of $z$ and (2.3) reduces to a simple, two-dimensional Laplace equation

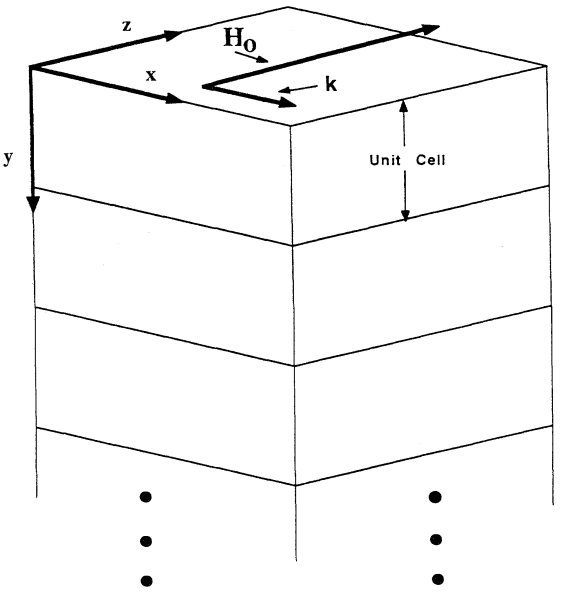


FIG. 1. The geometry considered in this paper. We examine a semi-infinite stack of unit cells, as shown, where the $y$ axis points into the structure, the applied magnetic field is along $z$, and the propagation is along $x$.

$$\left[\frac{\partial^2}{\partial x^2}+\frac{\partial^2}{\partial y^2}\right]\phi=0\ . \tag{2.4}$$

If we now imagine numbering the individual bilayers within a unit cell of the superlattice, and examine the $i$th bilayer in the $n$th unit cell, we may write solutions to (2.4) as follows:

$$\begin{aligned}\phi_{Ai}&=(A_{i+}e^{k\delta_y}+A_{i-}e^{-k\delta_y})e^{i(kx-\omega t)}e^{iQnL}\ ,\\ \phi_{Bi}&=(B_{i+}e^{k\delta_y}+B_{i-}e^{-k\delta_y})e^{i(kx-\omega t)}e^{iQnL}\ ,\end{aligned} \tag{2.5}$$

where $Q$ is the Bloch wave vector which relates the phase of the waves in unit cell $n$ to the phase of the waves in the neighboring unit cells, $L$ is the length of a unit cell, $\delta_y$ measures the distance along the $y$ axis within an individual layer, and the amplitudes $A$ and $B$ refer to the respective materials $A$ and $B$ comprising each bilayer.

At this point, we may construct a transfer matrix $\mathbf{T}$ which will give the potentials in the bilayer $i+1$ in terms of the potentials in bilayer $i$. To do so, we match boundary conditions (continuity of the potential and the normal component of $\mathbf{D}$) across the interfaces between materials $A$ and $B$ within a bilayer, and then across the interface with the next bilayer. Thus

$$\begin{aligned}&A_{i+}e^{kd_{Ai}}+A_{i-}e^{-kd_{Ai}}=B_{i+}+B_{i-}\ ,\\ &(-\epsilon_2+\epsilon_1)A_{i+}e^{kd_{Ai}}+(-\epsilon_2-\epsilon_1)A_{i-}e^{-kd_{Ai}}\\ &\qquad=\epsilon_B(B_{i+}-B_{i-})\end{aligned} \tag{2.6}$$

across the interface *within* bilayer $i$, and

$$B_{i+}e^{kd_{Bi}}+B_{i-}e^{-kd_{Bi}}=A_{(i+1)+}+A_{(i+1)-}\ ,$$
$$\epsilon_B(B_{i+}e^{kd_{Bi}}-B_{i-}e^{-kd_{Bi}})=(-\epsilon_2+\epsilon_1)A_{(i+1)+}+(-\epsilon_2-\epsilon_1)A_{(i+1)-} \tag{2.7}$$

across the interface *between* bilayer $i$ and bilayer $i+1$. Here, $d_{Ai}$ is the thickness of material $A$ in bilayer $i$, and $d_{Bi}$ is the thickness of material $B$. Each pair of equations (2.6) and (2.7) may be written in matrix form, which will give two matrix equations involving all of the amplitudes $A$ and $B$. A bit of matrix algebra allows us to eliminate the $B$'s, leaving

$$\vec{A}_{i+1}=\overleftrightarrow{T}\vec{A}_i\ , \tag{2.8}$$

where

$$\vec{A}_{i+1}=\begin{bmatrix}A_{(i+1)+}\\A_{(i+1)-}\end{bmatrix},\quad \vec{A}_i=\begin{bmatrix}A_{i+}\\A_{i-}\end{bmatrix},$$

$$\overleftrightarrow{T}=\frac{1}{4\epsilon_1\epsilon_B}\begin{bmatrix}[(\epsilon_2+\epsilon_1)(we_B^+ +ye_B^-)+\epsilon_b(we_B^+ -ye_B^-)]e_A^+ & [(\epsilon_2+\epsilon_1)(xe_B^+ -ze_B^-)+\epsilon_B(xe_B^+ -ze_B^-)]e_A^-\\ [(\epsilon_1-\epsilon_2)(we_B^+ +ye_B^-)-\epsilon_B(we_B^+ -ye_B^-)]e_A^+ & [(\epsilon_1-\epsilon_2)(xe_B^+ +ze_B^-)-\epsilon_B(xe_B^+ -ze_B^-)]e_A^-\end{bmatrix},$$

and where

$$w=\epsilon_B-\epsilon_2+\epsilon_1,\quad x=\epsilon_B-\epsilon_1-\epsilon_2\ ,$$
$$y=\epsilon_B-\epsilon_1+\epsilon_2,\quad z=\epsilon_B+\epsilon_1+\epsilon_2\ ,$$

and

$$e_B^+=e^{kd_{Bi}},\quad e_B^-=e^{-kd_{Bi}}\ ,$$
$$e_A^+=e^{kd_{Ai}},\quad e_A^-=e^{-kd_{Ai}}\ .$$

Note that the transfer matrix **T** depends upon the thicknesses $d_{Ai}$ and $d_{Bi}$. Therefore we may multiply $G_m$ transfer matrices together, inserting different thicknesses, in order to create another transfer matrix which will link the potentials in the first film of a unit cell with the first film in the next unit cell. Therefore we write

$$\overleftrightarrow{M}=\prod_{i=1}^{F_m}\overleftrightarrow{T}(d_i)\ . \tag{2.9}$$

If we now consider a superlattice consisting of an array of unit cells constructed as above, we arrive at the usual expression for the bulk dispersion relation[11] in terms of the transfer matrix **M**:

$$\cos(QL)=\tfrac{1}{2}\mathrm{Tr}\overleftrightarrow{M}\ , \tag{2.10}$$

where $Q$ is a Bloch wave vector governing the phase of the wave from one unit cell to the next, and $L$ is the length of the unit cell.

To find the dispersion for surface waves on the semi-infinite superlattice, we write the solution to (2.4) outside as $\phi=Ce^{ky}$, and then match the boundary conditions at the upper surface ($y=0$). Using this, along with an equation analogous to (2.10) for surface waves [replace $\cos(QL)$ by $\cosh(\beta L)$, with $\mathrm{Re}(\beta)>0$, to ensure that we have exponential decay into the material and hence a surface wave] we arrive at the dispersion for surface plasmons:

$$\lambda(M_{11}+\lambda M_{12})=M_{21}+\lambda M_{22}\ , \tag{2.11}$$

where

$$\lambda=\frac{\epsilon_1-\epsilon_2-\sigma\epsilon_0}{\epsilon_1+\epsilon_2+\sigma\epsilon_0}\ \text{and}\ \sigma=\frac{|k|}{k}\ ,$$

and $\epsilon_0$ is the dielectric constant of the medium above the superlattice.

In the next section, we will provide a specific numerical example of the above dispersion relations for a particular geometry.

## III. NUMERICAL EXAMPLES

In this section, we present numerical examples of dispersion relations and amplitude profiles of magnetoplasmons in semi-infinite Fibonacci superlattices. We will show that the effect of the quasiperiodic layering is to increase the number of bulk bands and surface modes, and also show that the new surface modes are nonreciprocal with respect to propagation direction in the presence of an applied magnetic field. In all of what follows, we assume that material $A$ is doped GaAs, while material $B$ is undoped GaAs. For these materials, then, we use $\epsilon_\infty=13.13$, and with a doping concentration of $n=10^{18}\ \mathrm{cm}^{-3}$, we calculate a plasma frequency of $\omega_p=0.040\,75$ eV.

We assume that there are two different thicknesses of bilayers which are arranged in a Fibonacci sequence to form unit cells. In particular, we will investigate a superlattice composed of a semi-infinite stack of unit cells, and each unit cell contains $G_3=3$ bilayers. If we label the two different bilayers $\alpha$ and $\beta$, then a unit cell composed of three bilayers will look like $\alpha\beta\alpha$. The total thickness of each bilayer will be denoted $d_\alpha$ and $d_\beta$, respectively, and we label the thicknesses of the *individual* films $d_{\alpha A}$, $d_{\alpha B}$, $d_{\beta A}$, and $d_{\beta B}$. The unit cell is shown in Fig. 2. In all of what follows, we take $d_\alpha/d_\beta=1.618$ (golden mean, as discussed in Sec. I), $d_{\alpha A}=2d_{\alpha B}$, and $d_{\beta A}=2d_{\beta B}$.

For the purpose of comparison, we begin by showing the dispersion curves for the periodic superlattice—

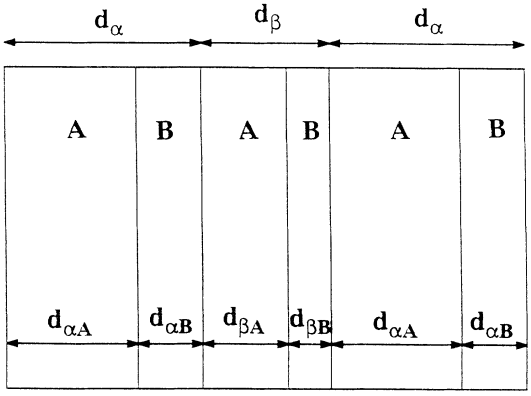


FIG. 2. The internal structure of the unit cell. We consider $F_3=3$, as explained in the text, so we have three different bilayers, two of thickness $d_\alpha$ and one of thickness $d_\beta$, as shown. The individual films have thicknesses as shown. Material $A$ has free charge, and material $B$ is an insulator.

$G_1=1$—in Fig. 3. The applied field is zero. The bulk bands are the cross-hatched regions, and the surface modes are the heavy lines. In this case the unit cell consists of a single bilayer, so we get two bulk bands and two surface modes.

In Fig. 4 we show the dispersion curves for bulk plasmons in the case $G_3=3$. Here we take the applied magnetic field to be zero. We see that there are six bulk bands in this case, as explained in Sec. I, since each bulk band which appears in the periodic case has split into $G_3=3$ bulk bands [the number of distinct active layers/(unit cell)]. The uppermost and lowermost bands are extremely narrow—note that the boundaries of the bulk bands are given by $QL=0$ and $QL=\pi$, as shown on the graph.

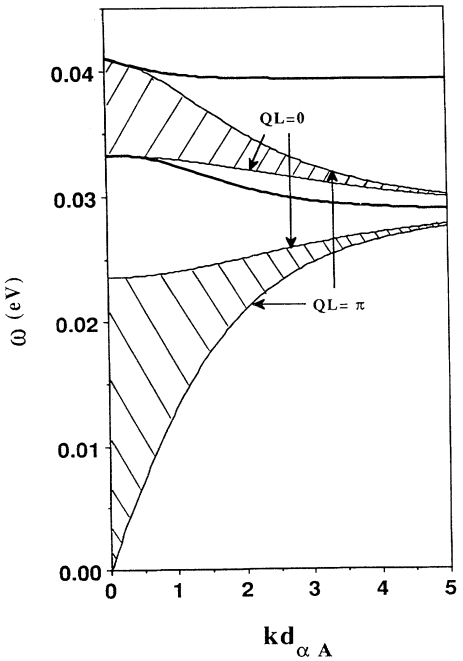


FIG. 3. The dispersion curves for the periodic superlattice ($F_1=1$). The bulk bands are the cross-hatched regions, while the surface modes are indicated by heavy lines.

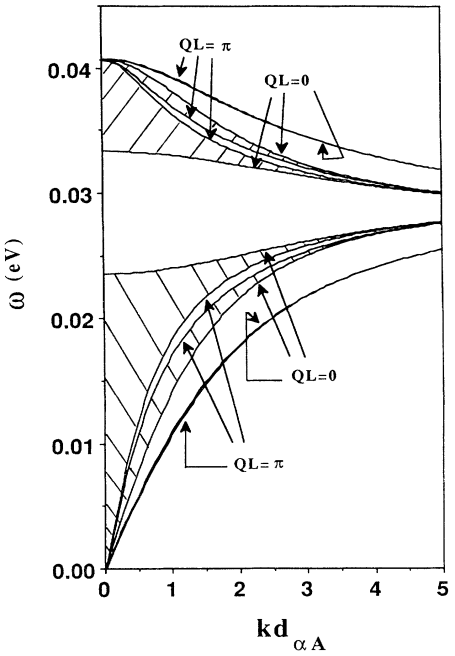


FIG. 4. The bulk dispersion curves for the quasiperiodic superlattice which is constructed of unit cells as pictured in Fig. 2. The magnetic field is zero. We note that each of the bands in Fig. 3 has been split into $F_3=3$ distinct bands, as explained in the text.

Figure 5 depicts the surface modes for the same superlattice, again without an applied field. Both $\pm k$ are shown, and we note that all modes are reciprocal with respect to propagation direction. Again, six modes are present; there are now six distinct interfaces in the first unit cell, and we see a spectrum indicative of modes localized at each one.

In contrast, Fig. 6 shows the dispersion for the surface modes again, but this time with an applied field given by $\omega_c=4.075$ meV (roughly 7 kG in this case). Again, both $\pm k$ are shown, and there are several points of interest. The uppermost surface mode which appears in Fig. 4 has been split on the order of the cyclotron frequency, i.e., the $+k$ branch has been shifted upwards in frequency (above the plasma frequency), while the $-k$ branch has been shifted downwards in frequency. The $-k$ branch of the highest-frequency mode is shifted far enough downward that we see a repulsion of modes near $k=-1.8$.

We note that there is an interesting gap between the $+k$ and $-k$ branches at $k=0$ for the mode at $\omega\sim 0.031$ eV. The origin of this gap can be traced to the semi-infinite geometry and the application of a magnetic field. If, for example, we examine the simple case of a semi-infinite sample of material $A$, it can be shown that the dispersion relation for surface waves is given by[12]

$$1+2\epsilon_2\sin\theta+(\epsilon_2^2-\epsilon_1^2)\sin^2\theta-\epsilon_1\epsilon_3\cos^2\theta=0 \qquad (3.1)$$

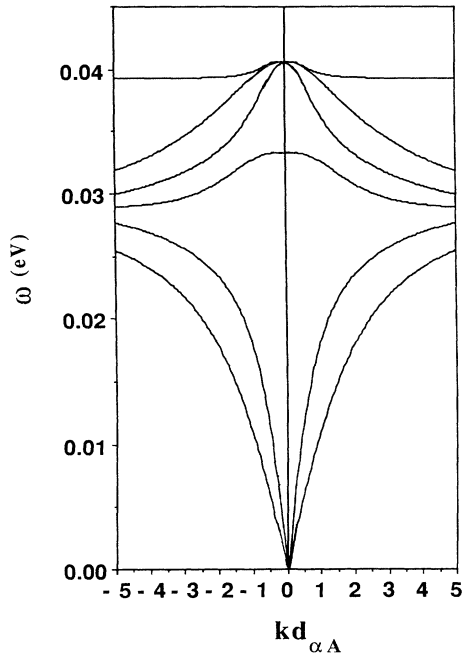


FIG. 5. The surface mode dispersion relations for the same structure as Fig. 4. Again, there is no magnetic field, and we note that the modes are reciprocal with respect to propagation direction. There are six modes, corresponding to the six distinct surfaces in the first unit cell.

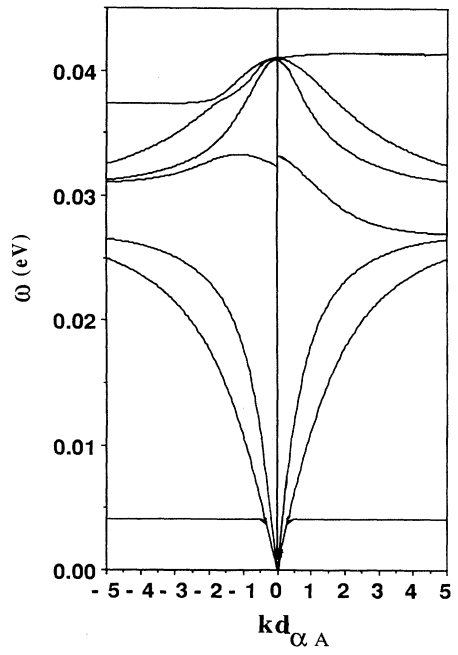


FIG. 6. The surface mode dispersion for the quasiperiodic superlattice in the presence of an applied magnetic field given by $\omega_c = 0.004\,075$ eV. Note the large degree of nonreciprocity present. Also note the gap in frequency between $+k$ and $-k$ solutions for $k=0$ at $\omega \sim 0.031$ eV.

where $\theta$ is the angle between $k_\parallel$ and the magnetic field, and the dielectric constants are defined as in Sec. II. We note that $\omega$ is independent of the magnitude of $k$ in this geometry and that $\omega$ (the frequency of the surface mode) lies between 0 and the plasma frequency $\omega_p$. The case of $+k$ is then given by $\theta = +90°$, while $-k$ is given by $\theta = -90°$. The dispersion relations corresponding to the two directions of propagation are then given by

$$\epsilon_1^2 - \epsilon_2^2 = 1 + 2\epsilon_2 \quad \text{for } +k \ ,$$

$$\epsilon_1^2 - \epsilon_2^2 = 1 - 2\epsilon_2 \quad \text{for } -k \ ,$$

and as a result of the different signs associated with $\epsilon_2$, a gap occurs. If we now consider a *finite* slab of material $A$, the boundary conditions then contain explicitly a length scale for the problem—i.e., the thickness of the slab appears in the boundary conditions. In this case, the dispersion relations are not independent of the magnitude of $k$, and the surface mode does not intersect the frequency axis between $\omega = 0$ and $\omega_p$ as $k \to 0$, but goes to either $\omega = 0$ or $\omega = \omega_p$ as $k \to 0$. Therefore the gap in the semi-infinite geometry becomes a large asymmetry (for $k \neq 0$) in the finite geometry. This is also the case for superlattices. In the semi-infinite superlattice, there exist surface modes which intersect the frequency axis between $\omega = 0$ and $\omega_p$.[13] However, in the finite superlattice the same surface modes either go to $\omega = 0$ as $k \to 0$, or to $\omega = \omega_p$ as $k \to 0$.[14] As we will see later, the $+k$ and $-k$ solutions near $k = 0$ are physically very different and thus a gap is not unreasonable.

Finally, we point out in Fig. 6 the emergence of an additional mode at the cyclotron frequency, which is associated with a degenerate bulk band. It can be shown that, in the generalized geometry which allows propagation at arbitrary angles with respect to the magnetic field, a bulk band emerges with applied field which runs from zero frequency up to the cyclotron frequency, but which gets narrower and eventually becomes degenerate when the propagation direction is perpendicular to the field. All of the modes shown in Fig. 5 are nonreciprocal, except for the mode associated with the bulk band at the cyclotron frequency.

It is illustrative to look at the amplitude profiles of the various plasmon modes in the Fibonacci-layered surface. For instance, we may wish to find out the differences, if any, between the $+k$ and $-k$ solutions for the middle set of surface modes ($\omega \sim 0.031$ eV) in Fig. 6. The amplitude profile (the amplitude of the potential $\phi$ as a function of depth into the superlattice) for this mode on the $+k$ branch is shown in Fig. 7(a). Here $kd_{\alpha A} = +3$, $\omega = 0.27\,64$ eV, and $\omega_c = 0.004\,075$ eV. The dashed lines indicate the boundaries between individual films, and a total of two unit cells are pictured. Note that the mode decays almost entirely within the first unit cell, and that its character is odd. Figure 7(b) depicts the amplitude profile for the mode at $\omega = 0.031$ eV, $kd_{\alpha A} = -3$, and the applied field is the same. Here we see the mode penetrating slightly further into the superlattice and it has even character. Note that this mode and the mode in Fig. 7(a) are most strongly localized to the top surface of the su-

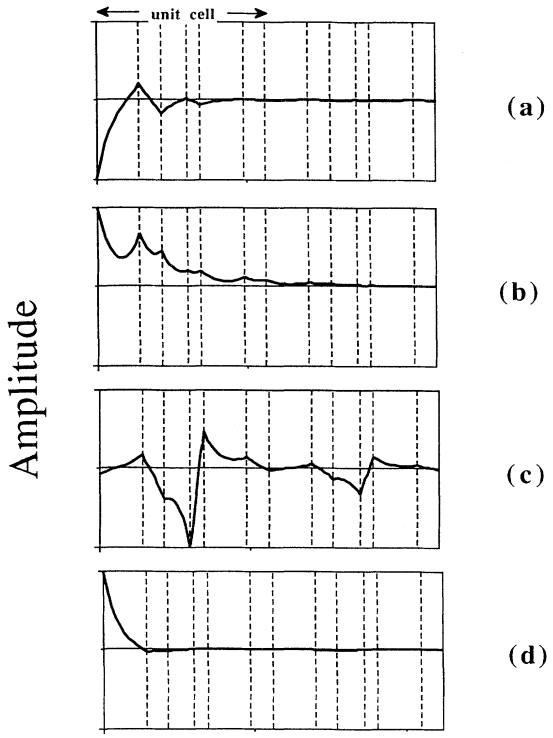


FIG. 7. The amplitude of the potential $\phi$ as a function of depth into the superlattice for four different surface modes. The dashed lines indicate the boundaries between individual films. Note that two unit cells are shown. In all graphs, we take $\omega_c = 0.004\,075$ eV (cf. Fig. 6). In (a), $kd_{\alpha A} = +3$, $\omega = 0.0276$ eV. Note the odd character of the mode. In (b), $kd_{\alpha A} = -3$, $\omega = 0.031$ eV. This is the $-k$ branch of the same mode as in (a). Here we see even character, and both (a) and (b) are localized at the outer surface. In (c), $kd_{\alpha A} = +3$, $\omega = 0.0215$ eV. This mode is localized at the fourth boundary into the top unit cell. In (d), $kd_{\alpha A} = -3$, $\omega = 0.0276$ eV. The mode is very strongly localized within the uppermost film.

perlattice, and therefore it is not surprising that a mode of nearly the same frequency exists in the periodic case.

A number of other surface modes deserve additional attention. For example, one of the modes not present in the periodic case is at $kd_{\alpha A} = 3$, $\omega = 0.0215$ eV, which exists in the gap between bulk bands at this frequency in Fig. 4. The amplitude profile for this mode is shown in Fig. 7(c). Note that it is most strongly localized at the fourth interface into the first unit cell, and that it extends further into the superlattice. In fact, the rather large value of $k$ ($kd_{\alpha A} = 3$) for this graph tends to limit the depth of penetration into the superlattice, and that for small values of $k$ the mode will extend even further. Finally, in Fig. 7(d), we examine the uppermost surface mode. Here we show the amplitude profile for $kd_{\alpha A} = -3$, $\omega = 0.0373$ eV, and $\omega_c = 0.004\,075$ eV. This mode is localized almost entirely within the uppermost *film*, and does not even appreciably penetrate the first unit cell. The high-frequency modes, then, are roughly independent of the layering in the unit cell.

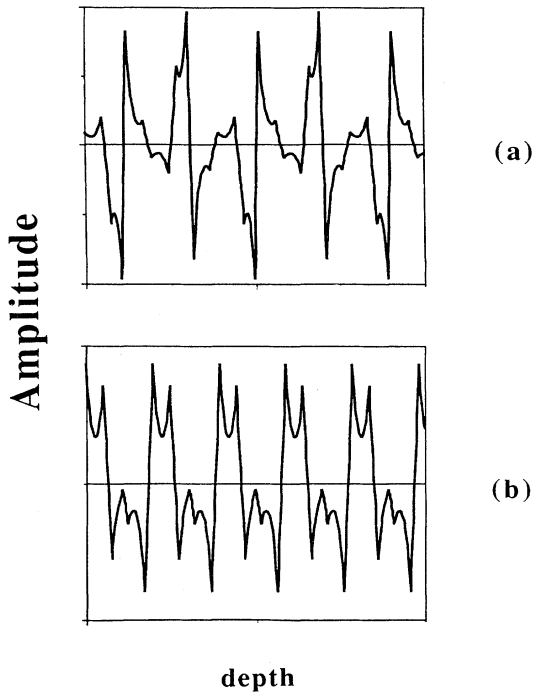


FIG. 8. The amplitude profile as a function of depth over five unit cells for bulk modes in the quasiperiodic superlattice. Here $H_0 = 0$. In (a), we show the mode $kd_{\alpha A} = 3$, $\omega = 0.0217$ eV visible in Fig. 4. The mode has a repeat distance of two unit cells. In (b), $kd_{\alpha A} = 3$, $\omega = 0.0246$ eV. Here the mode has a repeat distance of 1 unit cell.

Lastly, we show the amplitude profiles for bulk modes in the quasiperiodic system over five complete unit cells in Fig. 8. In both graphs, $H_0 = 0$. In Fig. 8(a) we show a mode at $kd_{\alpha A} = 3$, $\omega = 0.0217$ eV. The character of this mode is clearly bulk, with a repeat distance of two unit cells—note that just over two complete patterns are visible. In contrast, the mode shown in Fig. 8(b), for $kd_{\alpha A} = 3$, $\omega = 0.0246$ eV, shows a repeat distance of one unit cell, and five complete patterns are visible.

## IV. SUMMARY

We have investigated the dispersion relations and amplitude profiles of magnetoplasmons propagating in a semi-infinite quasiperiodic superlattice. We have examined a superlattice whose unit cells are composed of two different thicknesses of bilayers which are arranged in a Fibonacci sequence; specifically, we have looked at a unit cell composed of three bilayers—two of one thickness separated by a third of a different thickness. We have shown that there exist new additional bulk and surface plasmons in the quasiperiodic structure which do not exist in the periodic case, and that these surface modes show nonreciprocity in frequency with respect to direction of propagation. The structure of the amplitude profiles of these surface modes indicates that they are localized at the new interfaces, as expected.

## ACKNOWLEDGMENT

This work was supported by the Army Research Office, under Grant No. DAAL03-88-K-0061.

[1]M. Kohmoto, L. P. Kadanoff, and C. Tang, Phys. Rev. Lett. **50**, 1870 (1983).
[2]M. Kohmot, Phys. Rev. Lett. **51**, 1198 (1983).
[3]G. Gumbs and M. K. Ali, Phys. Rev. Lett. **60**, 1081 (1988).
[4]M. K. Ali and G. Gumbs, Phys. Rev. B **38**, 7091 (1988).
[5]P. Hawrylak and J. J. Quinn, Phys. Rev. Lett. **57**, 308 (1986).
[6]S. Das Sarma, A. Kobayashi, and R. E. Prange, Phys. Rev. Lett. **56**, 1280 (1986).
[7]M. Kolar and M. K. Ali, Phys. Rev. B **39**, 426 (1989).
[8]D.-H. Huang, J.-P. Peng, and S. Zhou, Phys. Rev. B **40**, 7754 (1989).
[9]A. P. Mayer, J. Phys. Condens. Matter **1**, 3301 (1989).
[10]B. L. Johnson and R. E. Camley, Phys. Rev. B **38**, 3311 (1988).
[11]For an example of the derivation of Eq. (2.10), see G. A. Farias, M. M. Auto, and E. L. Albuquerque, Phys. Rev. B **38**, 12 540 (1988).
[12]R. E. Camley, Surf. Sci. Rep. **7**, 103 (1987).
[13]R. E. Camley and D. L. Mills, Phys. Rev. B **29**, 1695 (1984).
[14]B. L. Johnson, J. T. Weiler, and R. E. Camley, Phys. Rev. B **32**, 6544 (1985).